DOI: https://doi.org/10.30898/1684-1719.2024.4.9

HIGH-TEMPERATURE TREATMENT OF FUNCTIONAL HEUSLER ALLOY $Ni_{46}Mn_{41}In_{13}$ THIN FOILS FOR MICROSYSTEM DEVICES AND ELECTRONICS

D.D. Kuznetsov[1], E.I. Kuznetsova[2], D.V. Danilov[3], I.I. Musabirov[4], A.V. Prokunin[1], V.V. Koledov[1], V.G. Shavrov[1]

[1] Kotelnikov IRE RAS, 125009, Russia, Moscow
[2] M.N. Mikheev Institute of Metal Physics of Ural Branch RAS 620108, Russia, Ekaterinburg
[3] IRC for Nanotechnology of the Science Park of St. Petersburg State University 199034, Russia, St. Petersburg
[4] Institute for Metals Superplasticity Problems RAS 450001, Russia, Ufa

The paper was received March 20, 2024.

Abstract. In this study, the high-temperature transformation in a thin foil of non-stoichiometric Heusler alloy based on Ni-Mn-In is investigated using *in-situ* TEM. The highly ordered cubic $L2_1$ phase undergoes decomposition upon heating, forming a phase with a composition close to $Ni_{75}Mn_{25}$, which is identified as disordered FCC-Ni_3Mn and secondary phases, mainly manganese oxides and sulfides. All phases formed upon heating to a temperature of 1173 K are preserved during the *in-situ* cooling experiment to a temperature of 123 K.

Key words: phase transformation, phase stability, size effects.

Financing: 1. The work was carried out with partial support from the state assignment of the IRE Kotelnikova RAS; 2. The work was carried out with partial support from the state assignment of the M.N. Mikheev Institute of Physics of Metals, Ural Branch of the Russian Academy of Sciences, code "Pressure" G.r. № 122021000032-5; 3. The preparation of foils and electron microscopic studies were carried out with the support

of St. Petersburg State University, project code AAAA-A19-119091190094-6; 4. Alloy ingots were melted as part of the state assignment of the IPSM RAS.

Corresponding author: Kuznetsov Dmitry Dmitrievich, Kuznetsov.dmitry89@gmail.com

Introduction

Shape memory alloys (SMA) that undergo thermoelastic martensitic transformation are an important class of metallic functional materials. The development of SMA has achieved significant success in solving practical problems in instrument engineering, medicine, micro- and nanosystem technology, etc. [1-10]. The properties of SMA strongly depend on the composition, processing, and microstructure. In addition, phase transitions in these materials also depend on the sample size [9], so when developing new functional SMA for micro- and nanosystem technology, size effects need to be taken into account. Size effects can influence the temperature and other characteristics of transformation in alloys, such as ordering and phase stability, which may subsequently be responsible for the existence of intermediate products, both thermodynamically equilibrium and metastable, not realized in bulk material [11-14]. In works [14-16], it is shown how heat treatment affects the microstructure of Ni-Mn-In system alloys, and the microstructure on phase transformations and, as a result, on SMA. An important issue remains the thermal stability (resistance of the material's structure to heating – preservation of all and/or its main properties) of both bulk and micro-, nanoscale materials for use in various radio electronic systems that use these alloys as a functional element - from contacts to active and passive cooling systems. Heusler alloys are increasingly being studied for use in spintronics [17-19].

In-situ phase transformation studies using electron microscopy methods: scanning (SEM), transmission (TEM), high-resolution TEM, in combination with heating, provide a unique opportunity for direct observation of the alloy structure during high-temperature transformations and the influence of the "thin foil" size effect

on the possible change in the nature of processes. Visualization is useful for identifying metastable states that may remain unnoticed in bulk systems. The object of study in this work is the $Ni_{46}Mn_{41}In_{13}$ alloy.

The aim of this work is to study the influence of high-temperature annealing on the microstructure and phase composition of the Heusler $Ni_{46}Mn_{41}In_{13}$ alloy. Special attention is paid to the characterization of the phase composition and evolution of the microstructure using transmission electron microscopy, including *in-situ* heating experiments in TEM, allowing direct monitoring of the analyzed phase transformations.

EXPERIMENTAL PROCEDURE

Polycrystalline samples of the $Ni_{46}Mn_{41}In_{13}$ alloy in the form of ingots weighing about 30 g were prepared from high-purity source metals Ni, Mn, In (99.99%) by arc melting in an argon atmosphere on a cold hearth with three turnovers and remelting. For the purpose of homogenization, the ingots were annealed in a vacuum at a temperature of 1173 K for 2 hours followed by rapid cooling in water at 288 K (quenching). The nominal composition is $Ni_{46}Mn_{41}In_{13}$ (e/a = 7.86).

The microstructure of the samples was investigated in the temperature range of 123-1173 K using a transmission electron microscope (TEM) Carl Zeiss Libra 200FE (accelerating voltage 200 kV) with an energy OMEGA filter, an energy-dispersive X-ray radiation detector Oxford Instruments X-Max 80, and a two-axis cryoanalytical holder Gatan Model 636 with a temperature controller Model 900 SmartSet cold stage controller. Zeiss Merlin is a scanning electron microscope with a field emission cathode, a GEMINI-II electron optics column, and an oil-free vacuum system. In addition to secondary electron detectors In-lens SE and SE2, the microscope is equipped with a four-quadrant backscattered electron detector (AsB) and a backscattered electron detector with energy filtering (EsB). The analytical capabilities of the microscope are expanded by additional attachments for X-ray microanalysis Oxford Instruments INCAx-act and a system for registering backscattered electron diffraction (EBSD) Oxford Instruments CHANNEL5.

X-ray diffraction studies in the temperature range from 86 K to 573 K were carried out on a Rigaku Ultima IV multifunctional diffractometer using CuKα radiation, a graphite monochromator on a diffracted beam of a scintillation detector, and a low- and medium-temperature attachment LMT (Rigaku, Japan, Tokyo).

RESULTS AND DISCUSSION

Fig. 1 shows the X-Rayograms of the $Ni_{46}Mn_{41}In_{13}$ alloy annealed at a temperature of 1173 K for 2 hours followed by quenching. The X-ray diffractograms were analyzed using the space group $Fm\bar{3}m$. At room temperature, the alloy is in the austenitic state with FCC fundamental lattice reflections (220), (400) and (422) of the highly ordered phase $L2_1$. Moreover, the peak 200 $L2_1$/001 B2 is better expressed, a weak peak (111) $L2_1$ is observed, and peaks (311) and (331) are practically absent (high proportion of B2). At least up to a temperature of 353 K, the alloy is in the austenitic state with fundamental lattice reflections (220), (400), and (422). The peak 200 $L2_1$/001 B2 is observed, peaks (111), (311), and (331) $L2_1$ are absent (very high proportion of B2). All peaks become less sharp after heating above T_c = 305 K and their intensity decreases as a result of an increase in the frequency and amplitude of uncoordinated thermal vibrations of atoms.

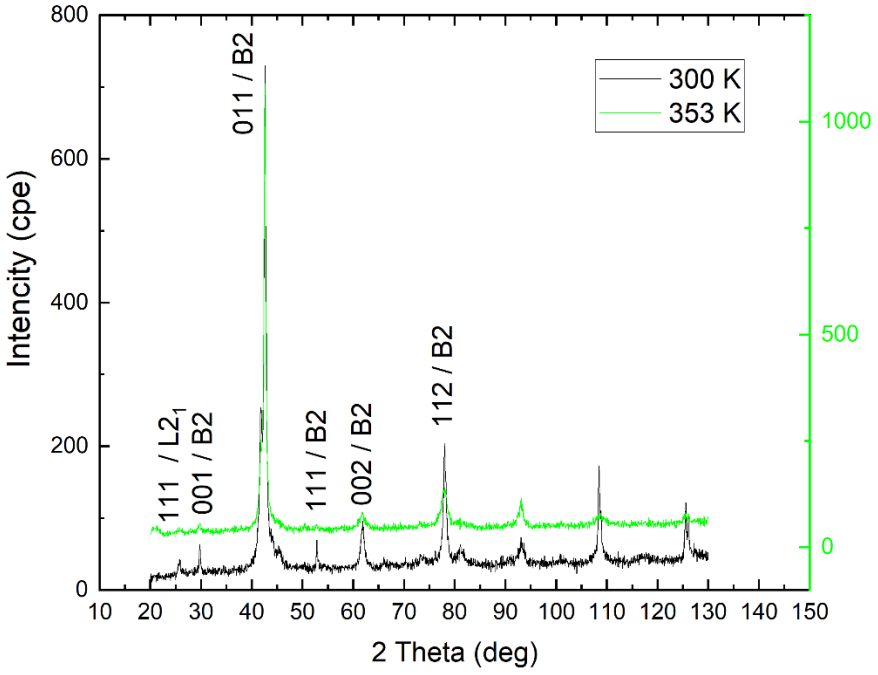

Fig. 1. X-ray diffractograms of the $Ni_{46}Mn_{41}In_{13}$ alloy at 300 K – room temperature (black line) and after heating to 353 K (green line).

To investigate transformations upon heating the alloy at the micro level, we conducted a series of *in-situ* experiments in a transmission electron microscope. At room temperature, the alloy is in the austenitic state, which is confirmed by X-Ray structural studies. The main diffraction spots (all diffraction patterns are indexed according to the $L2_1$ type ordering) belong to the cubic cell with a lattice parameter a = 0.608 nm (Fig. 2).

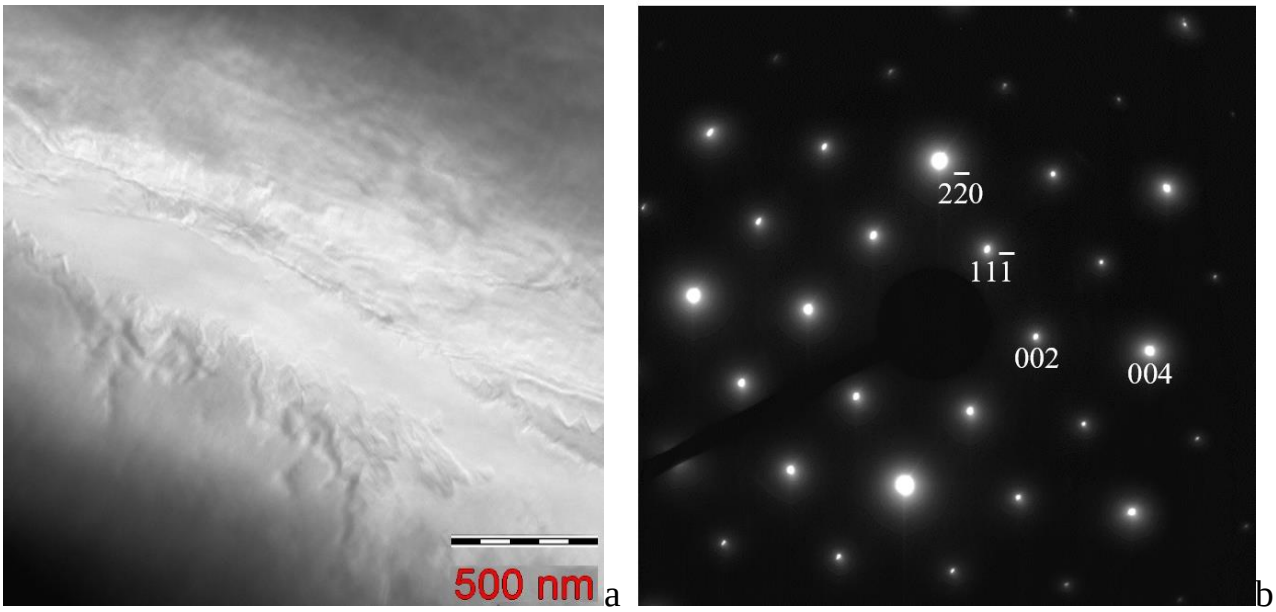

Fig. 2. Bright field image (a) and corresponding microelectronogram with the $[110]_{L21}$ zone axis (b). Observations at room temperature. All peaks are indexed according to the $L2_1$ type ordering.

The homogenization temperature of this alloy is 1173 K. We tried to conduct an *in-situ* TEM experiment with heating to this temperature. Upon heating the foil in the microscope column to 1173 K, the $L2_1$ structure of the Ni-Mn-In alloy degrades. A melting effect is observed – holes appear and increase in size, and a kind of eutectic with liquid is formed. The liquid leaks out, and flakes fall out at the edges of the holes (Fig. 3 a-c). Calculation of microdiffraction patterns showed that as a result, an FCC phase was formed with a lattice parameter a = 0.356 – 0.362 nm (Fig. 3g, d).

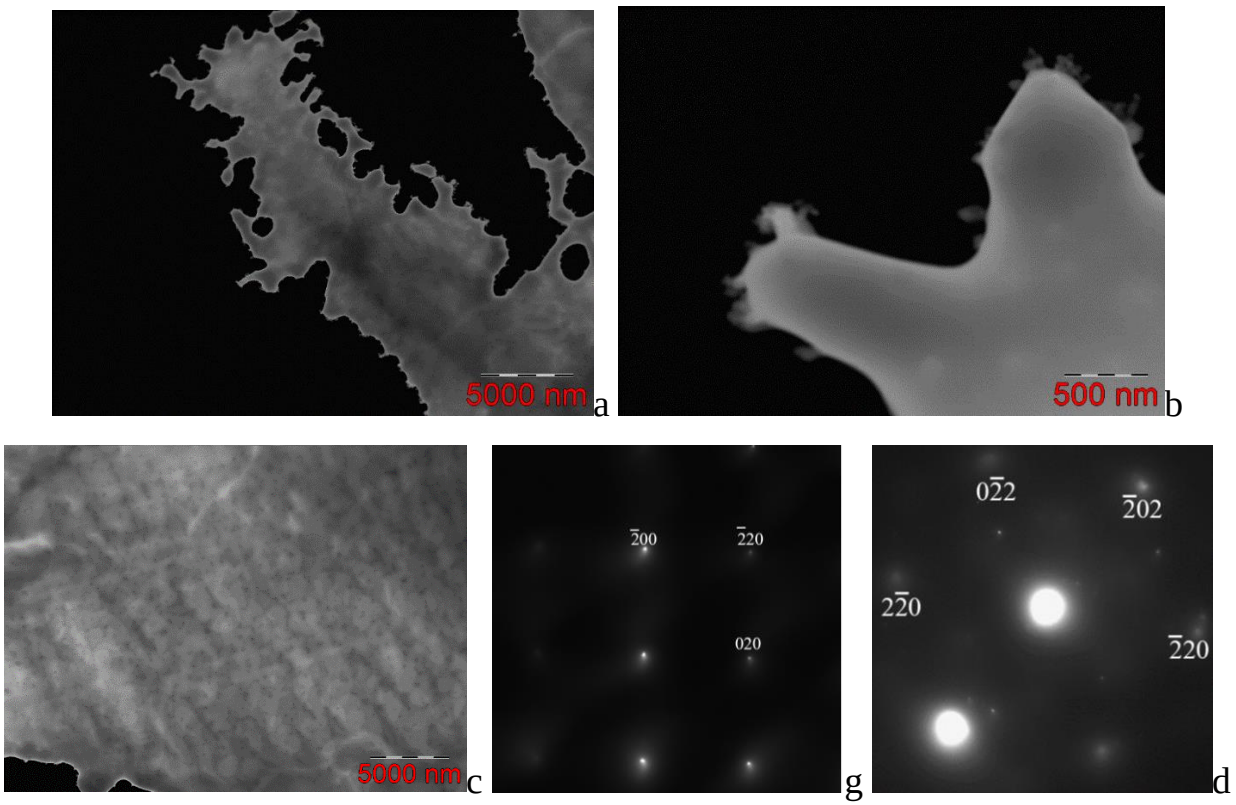

Fig. 3. a-c – HAADF images; g – microelectronogram with the $[001]_{FCC}$ zone axis, obtained from the area shown in Fig. 3c; d – microelectronogram with the $[111]_{FCC}$ zone axis, obtained when tilting the sample. Observations at 1173 K.

The chemical composition of the phase was estimated using EDX, conducted after cooling to room temperature. As can be seen from the distribution of elements along the scanning line, the sample showed a slight exit from the sample of Ni and a significant decrease in the content of In (Fig. 4). It should be noted that at a high heating rate, there is initially a temperature jump of 10-15 K before the sample temperature stabilizes. Such a temperature jump enhances the "leaching" of In from the system. The results of EDX indicate a composition of 72.33 – 74.04 at.% Ni and 27.67 – 25.96 at.% Mn, which is within the range of the composition of the Ni_3Mn phase (a = 0.358 nm). Fig. 4b shows the concentration profiles of Ni, Mn, and In (concentration C is plotted as a function of position x). Mapping in the characteristic X-Ray spectra of these chemical elements is shown in Fig. 4c.

It is believed that the Ni_3Mn phase transforms from the unstable NiMn phase during aging [20]. The exit of indium from the sample upon heating favors the formation of the NiMn phase, so possibly at lower temperatures, an ordered FCC-NiMn

phase is formed, which with increasing temperature (exit of magnesium) transforms into a disordered and more stable FCC-Ni_3Mn.

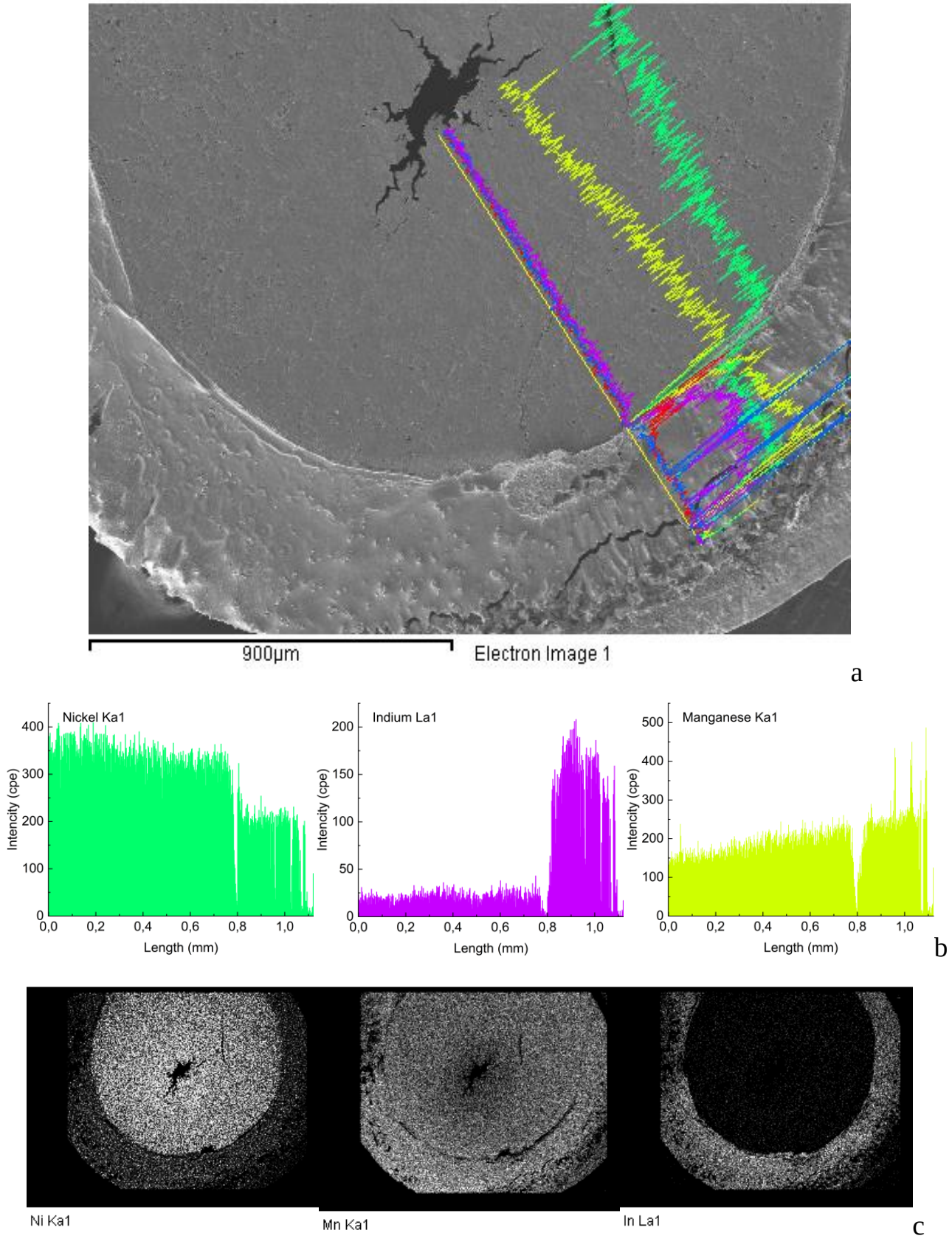

Fig. 4. SEM image (a), distribution of elements Ni, Mn, In along the scanning line (b) and maps of element distribution (c). Observations at room temperature.

Step-by-step observations were carried out in TEM to characterize the crystal structure of secondary phases crystallizing upon cooling from 1173 K. Figures 5 a,b show dark-field images in the matrix reflection and in the reflection of the second phase. Precipitates up to 400 nm in size are observed. Calculation of microdiffraction patterns correlates the second phase as an FCC structure with a lattice parameter a = 0.944 nm, which can be associated either with the cubic phase Mn_3In (a = 0.944 nm) or with the cubic phase Mn_2O_3 (a = 0.941 nm), which is the most stable form of manganese oxide at room temperature (Fig. 5c, lattice highlighted in red). The orientation relationship between the Ni_3Mn matrix and the secondary phase is $(001)_{Ni3Mn}//(120)$ and $[200]_{Ni3Mn}//[211]$. Microanalysis of the matrix using EDX showed that the atomic ratio Ni:Mn was approximately 73:27 (Fig. 6a, area highlighted in blue), which confirms the composition of Ni_3Mn. Thus, the system represents a mixture of two phases – Ni_3Mn matrix (cubic lattice) and the second phase (cubic lattice) with very differing parameters. In the matrix, a high concentration of dislocation loops is observed (Fig. 5a). Most of the detected large particles have an almost cubic shape and are located predominantly along the directions $[200]_{Ni3Mn}$ and $[020]_{Ni3Mn}$ of the matrix, which should be caused by minimizing stresses at the interface between the matrix and precipitates. EDS spectra showed that the main components – nickel and manganese are distributed evenly, and oxygen and impurity elements are localized in inclusions (Fig. 6a, area highlighted in red). In addition to dispersed oxides, manganese sulfides are observed, falling out in the form of flakes at the edges of holes, which apparently appeared due to the melting of the foil (Fig. 7). The Ni_3Mn phase is observed in the sample upon cooling, down to a temperature of 123 K, which is confirmed by the reflections of the FCC phase on microdiffraction patterns.

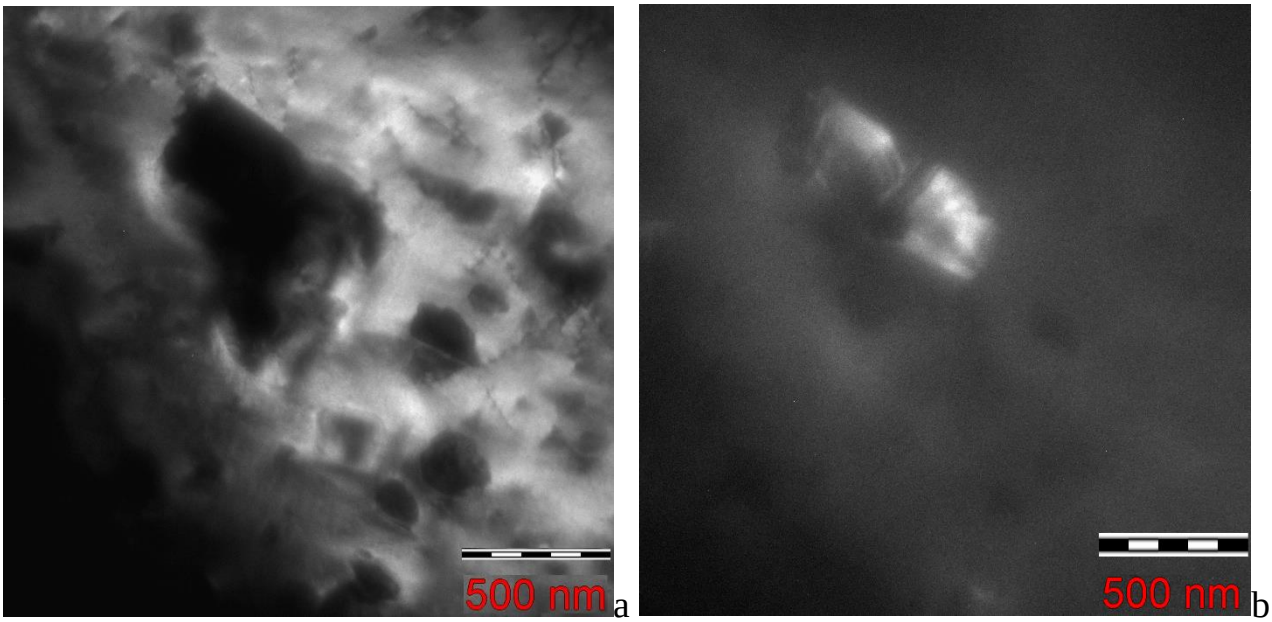

a b

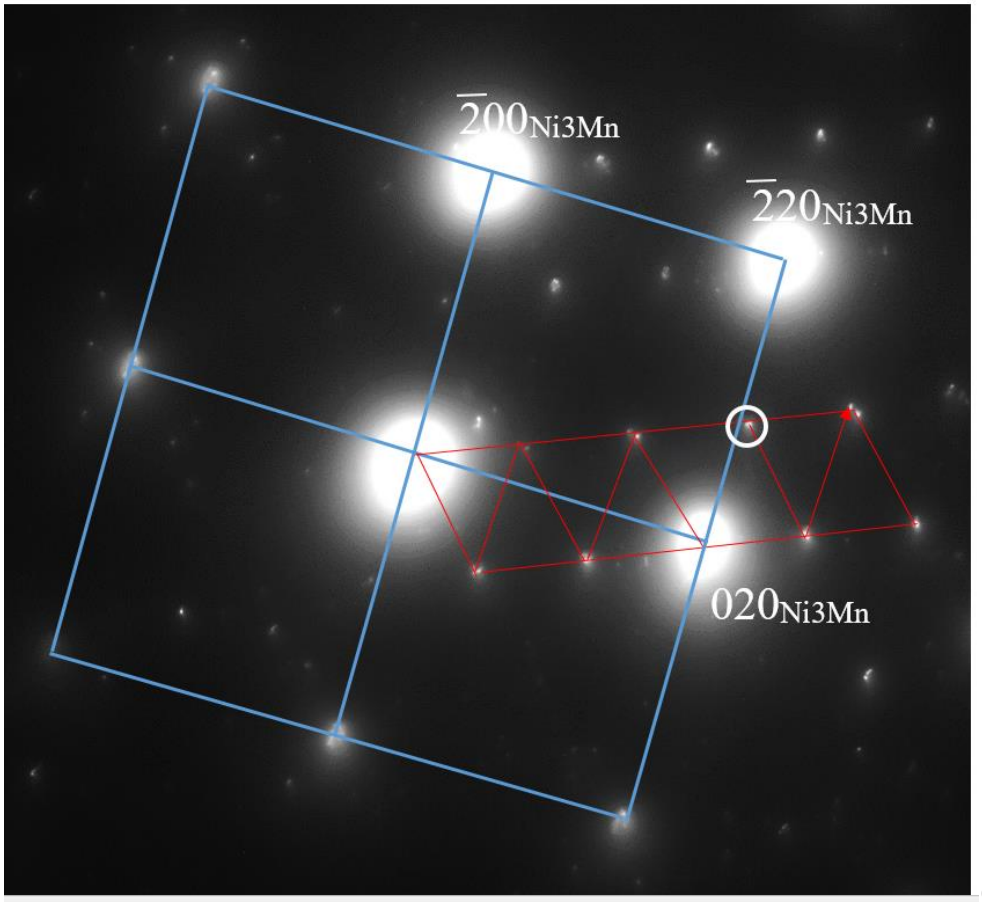

c

Fig. 5. Dark field images in the matrix reflection $\bar{2}00_{Ni3Mn}$ (a), in the reflection of the secondary phase (b, circled on the electronogram) and the corresponding microelectronogram (c) with the $[001]_{Ni3Mn}$ zone axis. Observations upon cooling to 373°C.

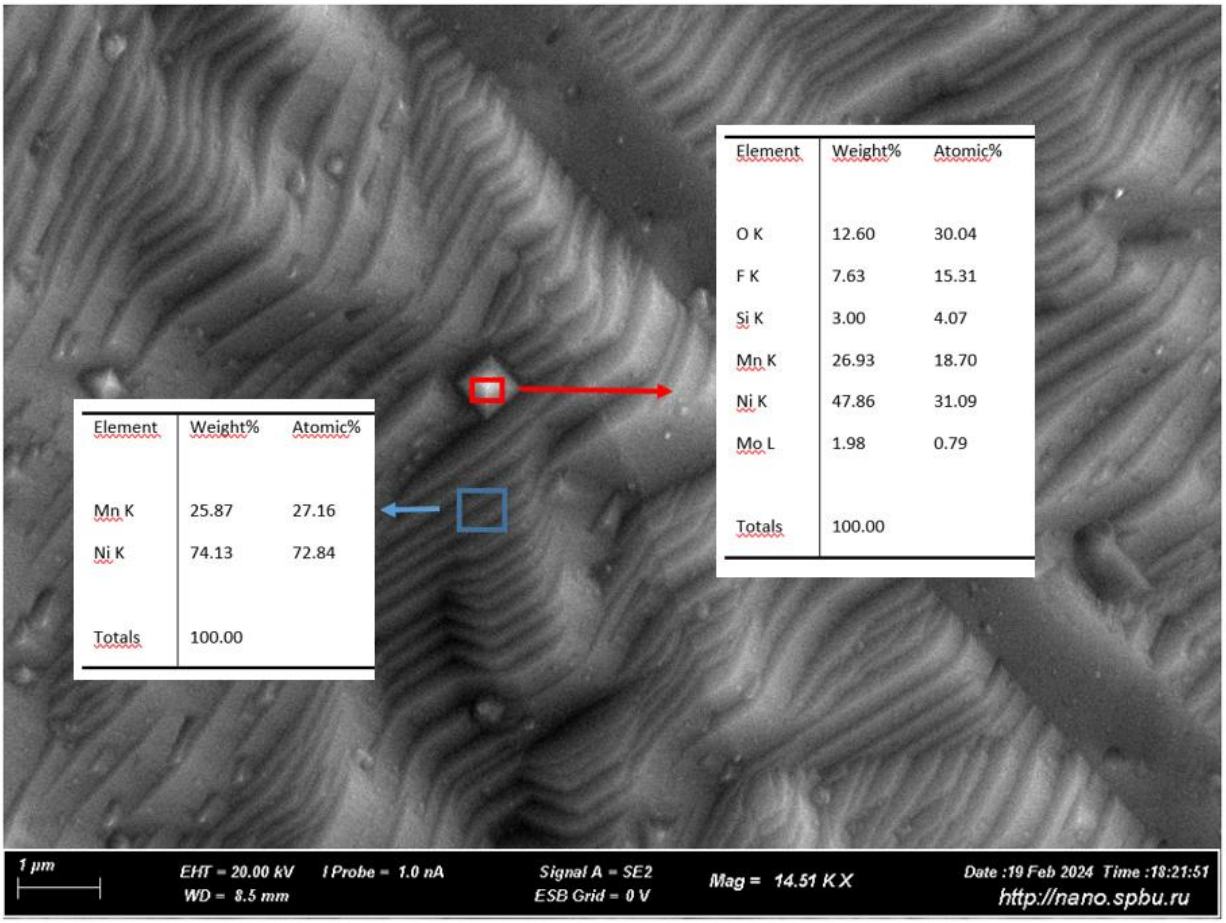

Fig. 6. SEM image and results of elemental analysis obtained from the matrix (left table) and the secondary phase (right table).

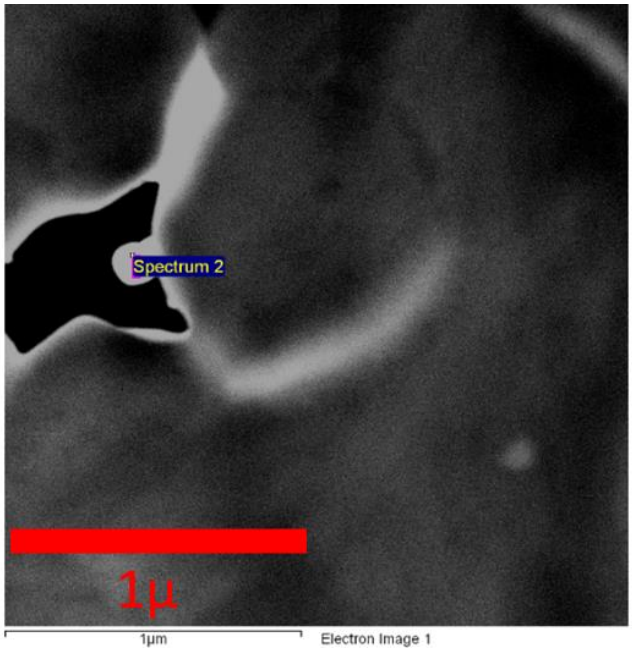

Element	Weight%	Atomic%
Al K	2.09	3.59
S K	23.48	33.92
Mn K	69.38	58.51
Ni K	5.05	3.98
Totals	100.00	

Fig. 7. Bright field TEM image and results of elemental analysis obtained from flakes falling out at the edges of holes.

Conclusion

In-situ heating and cooling experiments and diffraction pattern identification showed that when heated to a temperature 1170 K, the highly ordered cubic $L2_1$ phase based on Ni-Mn-In undergoes decomposition, due to partial melting and redistribution of nickel and manganese. The melting point of micro- and nanoscale foil was 1173 K. As a result, a matrix phase with a composition close to $Ni_{75}Mn_{25}$ is formed, which is identified as a disordered FCC-Ni_3Mn and secondary phases, mainly manganese oxides and sulfides. Thus, thermal treatment and/or operating temperature of micro- and nanoscale products should not be close to the melting temperature of thin foil, in order to prevent local melting of samples and excessive evaporation of indium and manganese, the appearance of oxides and sulfides.

Financing: 1. The work was carried out with partial support from the state assignment of the IRE Kotelnikova RAS; 2. The work was carried out with partial support from the state assignment of the M.N. Mikheev Institute of Physics of Metals, Ural Branch of the Russian Academy of Sciences, code "Pressure" G.r. № 122021000032-5; 3. The preparation of foils and electron microscopic studies were carried out with the support of St. Petersburg State University, project code AAAA-A19-119091190094-6; 4. Alloy ingots were melted as part of the state assignment of the IPSM RAS.

References

1. Wu M. H. et al. Industrial applications for shape memory alloys // Proceedings of the international conference on shape memory and superelastic technologies, Pacific Grove, California. – 2000. – V. 44. – №. 1.
2. Song C. History and current situation of shape memory alloys devices for minimally invasive surgery // The Open Medical Devices Journal. – 2010. – V. 2. – №. 1.
3. Cuschieri A. Variable curvature shape-memory spatula for laparoscopic surgery // Surgical endoscopy. – 1991. – V. 5. – P. 179-181.
4. Himpens J. M. Laparoscopic inguinal hernioplasty: repair with a conventional vs a new self-expandable mesh // Surgical endoscopy. – 1993. – V. 7. – P. 315-318.

5. Frank T., Willetts G. J., Cuschieri A. Detachable clamps for minimal access surgery // Proceedings of the Institution of Mechanical Engineers, Part H: Journal of Engineering in Medicine. – 1995. – V. 209. – №. 2. – P. 117-120.
6. Frank T. et al. Atraumatic retractor for endoscopic surgery // Surgical endoscopy. – 1995. – V. 9. – P. 841-843.
7. Liu J. et al. NiMn-based alloys and composites for magnetically controlled dampers and actuators // Advanced Engineering Materials. – 2012. – V. 14. – №. 8. – P. 653-667.
8. McHenry M. E., Laughlin D. E. Nano-scale materials development for future magnetic applications // Acta materialia. – 2000. – V. 48. – №. 1. – P. 223-238.
9. Lega P. et al. Blocking of the martensitic transition at the nanoscale in a Ti 2 NiCu wedge // Physical Review B. – 2020. – V. 101. – №. 21. – P. 214111.
10. Hirohata A., Lloyd D. C. Heusler alloys for metal spintronics // MRS Bulletin. – 2022. – V. 47. – №. 6. – P. 593-599.
11. Belo J. H. et al. Magnetocaloric materials: From micro-to nanoscale // Journal of Materials Research. – 2019. – V. 34. – №. 1. – P. 134-157.
12. Vishnoi R., Singhal R., Kaur D. Thickness dependent phase transformation of magnetron-sputtered Ni–Mn–Sn ferromagnetic shape memory alloy thin films // Journal of Nanoparticle Research. – 2011. – V. 13. – P. 3975-3990.
13. Teichert N. et al. Influence of film thickness and composition on the martensitic transformation in epitaxial Ni–Mn–Sn thin films // Acta Materialia. – 2015. – V. 86. – P. 279-285.
14. D. D. Kuznetsov, E. I. Kuznetsova, A. V. Mashirov, A. S. Loshachenko, D. V. Danilov, G. A. Shandryuk, V. G. Shavrov, V. V. Koledov In Situ TEM Study of Phase Transformations in Nonstoichiometric Ni46Mn41In13 Heusler Alloy // Physics of the Solid State. – 2022. – V. 64. – P. 15–21.
15. Kuznetsov D.D. et al. Magnetocaloric Effect, Structure, Spinodal Decomposition and Phase Transformations Heusler Alloy Ni-Mn-In // Nanomaterials . – 2023. – V. 13. – P. 1385–1402.

16. Kuznetsov D.D. et al. Influence of the Cooling Rate on Austenite Ordering and Martensite Transformation in a Non-Stoichiometric Alloy Based on Ni-Mn-In // Journal of Composites Science. – 2023. – V. 7. – P. 514–533.
17. Bainsla L., Suresh K.G. Equiatomic quaternary Heusler alloys: A material perspective for spintronic applications // Applied Physics Reviews. – 2016. – V. 3. – №. 3.
18. Elphick K. et al. Heusler alloys for spintronic devices: review on recent development and future perspectives // Science and technology of advanced materials. – 2021. – V. 22. – №. 1. – P. 235-271.
19. Arman M., Shahri F., Gholamipour R. Effect of Al doping on the kinetics of reverse martensitic transformation in Ni-Mn-In Heusler alloys //Materials Science and Engineering: B. – 2024. – V. 300. – P. 117068.
20. Е.С. Белослудцева, В.Г. Пушин, Н.Н. Куранова, Д.Е. Винокуров, О.А. Гусев Исследование фазовых превращений микроструктуры сплавов на основе бинарного сплава стехиометрического состава Ni-Mn // Межд. научно-технич. конф. «XXII Уральская школа-семинар металловедов – молодых ученых», Екатеринбург, 27.10.2023, ISBN: 978-5-91256-612-7, Сборник статей , Екатеринбург : УрФУ, 2023. – С. 311-315.

For citation:

Kuznetsov D.D., Kuznetsova E.I., Danilov D.V., Musabirov I.I., Prokunin A.V., Koledov V.V., Shavrov V.G. High-temperature treatment of functional heusler alloy $Ni_{46}Mn_{41}In_{13}$ thin foils for microsystem devices and electronics. // Journal of Radio Electronics. – 2024. – №. 4. https://doi.org/10.30898/1684-1719.2024.4.9